CONTRAST MEDIA & MOLECULAR IMAGING

Received: 4 May 2015, Revised: 9 July 2015, Accepted: 18 August 2015, Published online in Wiley Online Library: 14 October 2015

(wileyonlinelibrary.com) DOI: 10.1002/cmmi.1669

Compartmentalization of Gd liposomes: the quenching effect explained

Jamal Guenoun[a], Gabriela N. Doeswijk[a], Gabriel P. Krestin[a] and Monique R. Bernsen[a,b]*

Cationic liposomes carrying high [Gd] can be used as efficient cell-labeling agents. In a compartmentalized state, Gd can cause signal loss (relaxivity quenching). The contributions of liposomal [Gd], size and compartmentalization state to relaxivity quenching were assessed. The dependency of signal intensity (SI) on intraliposomal [Gd] was assessed comparing three different [Gd] (0.3, 0.6 and 1.0 M Gd) in both small (80 nm) and large (120 nm) cationic liposomes. In addition, five compartmentalization states were compared: free Gd, intact Gd liposomes, ruptured Gd liposomes, Gd liposomes in intact cells and Gd liposomes in ruptured cells (simulating cell death). Gd also causes R_2 effects, which is often overlooked. Therefore, both R_1 and R_2 relaxation rates of a dilution range were measured by T_1 and T_2 mapping on a 7 T clinical scanner. Less is more. As the unidirectional water efflux rate (outbound across the liposome membrane, κ_{le}) is proportional to the surface:volume ratio, smaller liposomes yielded a consistently higher R_1 than larger liposomes. For equal voxel [Gd] less concentrated liposomes (0.3 M Gd) yielded higher R_1/R_2 ratio because of the higher extraliposomal water fraction (v_l). Gd exhibits a dualistic behavior: from hypointensity to hyperintensity to hypointensity, with decreasing [Gd]. Regarding compartmentalization, fewer membrane barriers means a higher R_1/R_2 ratio. Gd liposomes exhibit a versatile contrast behavior, dependent on the compartmentalization state, liposomal size, intraliposomal [Gd] and liposome number. Both R1 and R2 effects contribute to this. The versatility allows one to tailor the optimal liposomal formulation to desired goals in cell labeling and tracking. Copyright © 2015 John Wiley & Sons, Ltd.

Keywords: cell labeling; quenching; MRI; Gd liposomes; gadolinium; liposomes; cell tracking

1. INTRODUCTION

Cellular imaging is the key to non-invasive assessment of cell transplantation therapies. In this rapidly evolving field many aspects of the *in vivo* kinetics of transplanted cells still need to be understood. Magnetic resonance imaging (MRI) provides excellent opportunities in this particular field thanks to its versatile properties. Combining the right ligand with an MR-sensitive contrast agent, magnetic resonance imaging is capable of exposing a wide range of previously visually occult *in vivo* molecular or cellular processes to the naked eye.

The two types of MRI contrast agent (CA) currently most widely used are T_1 agents (gadolinium (Gd) and to a lesser extent manganese (Mn)) or T_2 agents (iron oxide particles). Much (pre) clinical experience has been gained in the past decades with Gd-based contrast agents, for example Gd-DTPA (Magnevist, Schering, Germany) and Gd-DO3A-butrol (Gadovist, Schering). Their use as a cell labeling agent has however been limited, presumably because of the lower sensitivity obtained when compared with iron oxide particles. Nonetheless, cationic liposomes loaded with high concentrations of Gd can be used as an efficient cell-labeling agent for sensitive cellular MRI (1). Gd-based contrast agents have been used successfully in several other studies as well (2–7). As Gd mainly shortens T_1 relaxation times (and to a lesser extent T_2 relaxation times), its classical application consists of the generation of signal gain (hyperintense or positive contrast) on T_1-weighted images. Strikingly, in a compartmentalized (intracellular) state, Gd can cause signal loss (hypointense or negative contrast), known as 'relaxivity quenching' (3,7,8). Although initially thought of as a drawback (9), a recent study showed that contrast changes as a result of (de)quenching can be advantageous, allowing for a visual and quantitative distinction between viable and non-viable Gd-liposome-labeled cells by MRI (10). Relaxivity quenching thus might harbor more potential for cellular labeling than currently known. This at the time novel finding of dynamic contrast behavior *in vivo* encouraged us to study Gd signal quenching in more detail. The relaxivity of Gd is mainly affected by four parameters: the number of water molecules in the inner coordination sphere of the complex, the proton exchange rate in this inner sphere, the rotational correlation times (related to the size of the molecule) and the electron spin relaxation rates.

As encapsulation of Gd (inside liposomes and/or inside cells) affects the transmission of the effect of the paramagnetic center because of the liposome membrane and the possible restricted water exchange through this membrane, a better understanding of relaxivity (de)quenching could contribute to an enhanced

* *Correspondence to: M. R. Bernsen, Department of Radiology, Erasmus MC – University Medical Center Rotterdam, Rotterdam, The Netherlands. E mail: m.bernsen@erasmusmc.nl*

a *J. Guenoun, G. N. Doeswijk, G. P. Krestin, M. R. Bernsen*
Department of Radiology, Erasmus MC – University Medical Center Rotterdam, Rotterdam, The Netherlands

b *M. R. Bernsen*
Department of Nuclear Medicine, Erasmus MC – University Medical Center Rotterdam, Rotterdam, The Netherlands

image interpretation with regard to cell division, cell density and Gd-liposome load. No doubt this would further open up possibilities in image-guided monitoring of cell transplantation. Although most studies concerning Gd report merely T_1 longitudinal times, in the same study we observed that Gd compartmentalization (in liposomes) increased r_2 relaxivity (compared with 'free' Gd). Both T_1 and T_2 relaxation times of Gd-lipsomes and Gd-liposome-labeled cells were assessed, as signal intensity (SI) is dependent on both. Realizing that high payloads of CAs are involved in cell labeling, we focus on the high intraliposomal [Gd] concentrations (0.3 M–1.0 M Gd), which, to our knowledge, have not been studied before.

2. MATERIAL AND METHODS

2.1. Liposome preparation

As described before (1), cationic liposomes were prepared to serve as a vehicle to transfer Gd to cells. In brief, a 100 μmol mixture of 1,2-dipalmitoyl-*sn*-glycero-3-phosphocholine (DPPC; Lipoid, Ludwigshafen, Germany), cholesterol (Sigma-Aldrich, St Louis, MO, USA) and 1,2-dioleoyl-3-trimethylammonium-propane (chloride salt) (DOTAP; Avanti Polar Lipids, Alabaster, AL, USA) in the molar ratio 47:33:20 was dissolved in chloroform:methanol 2:1 (v:v). Gd-DO3A-butrol (Gadovist; Bayer Schering Pharma, Berlin, Germany) was incorporated in these liposomes using the lipid-film hydration technique followed by filtration through polycarbonate filters (Whatman, Newton, MA, USA).

2.2. Cell labeling and preparation

Firefly luciferase (Fluc-MSCs) of Passage 4 were used for all experiments. Dulbecco's modified Eagle's medium (Invitrogen; Carlsbad, CA, USA) enriched with additives was used as culture medium. In short, Fluc-MSCs were labeled with Gd liposomes, containing 125 μM lipid, for 4 h, harvested by trypsinization, washed three times in PBS and centrifuged at 300 *g* for 5 min to discard unincorporated contrast agent (1).

After centrifugation and cell counting, cells were resuspended to their final concentration in 1.07 g mL^{-1} Ficoll (*in vitro* experiments) or PBS (*in vivo* experiments).

2.3. Experiment 1: liposomal size and Gd load

To assess possible effects of liposomal size and liposomal Gd concentration on T_1 and T_2 relaxation times, varying liposomal formulations were prepared. Liposomes were encapsulated with Gd-DO3A-butrol (Gadovist 1.0 M) in three different intraliposomal Gd concentrations: 1.0 M Gd (undiluted), 0.6 M Gd and 0.3 M Gd, diluted in 4-(2-hydroxyethyl)-1-piperazineethanesulfonic acid (HEPES)-buffered saline (20 mM HEPES, 135 mM NaCl, pH adjusted to 7.4). From each batch, both large and small liposomes were created. Large liposomes were produced by filtering five times through 200 nm polycarbonate membrane filters followed by filtering five times through 100 nm filters. Smaller liposomes were created by five additional passes through 50 nm filters, followed by ultracentrifugation (300 000 *g* at 4 °C) to separate non-encapsulated from encapsulated Gd. Six different liposomal formulations were finally acquired: 1.0 M Gd with size 127 nm (1.0 M_L) and polydispersity index (PDI) 0.076, 1.0 M Gd with size 83 nm and PDI 0.054 (1.0 M_S), 0.6 Gd with size 119 nm and PDI 0.045 (0.6 M_L), 60% Gd with size 93 nm and PDI 0.069 (0.6 M_S), 30% Gd with size 124 nm and PDI 0.071 (0.3 M_L) and 30% Gd with size 91 nm and PDI 0.066 (0.3 M_S). The subscript abbreviations L and S refer to the sizes of the liposomal vesicles, with L indicating large and S indicating small. The average diameter and size distribution of the liposomes in the final formulation was determined by dynamic light scattering (DLS) using a Zetasizer Nano (Malvern Instruments, Malvern, Worcestershire, UK). Liposomal phosphorus content was assessed by spectrophotometric analysis according to Rouser *et al*. (11). As quenching occurs at high (intraliposomal) concentrations of Gd, we aimed to produce very concentrated Gd liposomes. To this end, the resulting liposome pellet of each batch was resuspended in 400 μL HEPES. A serial dilution of each suspension was then prepared and used to fill a 384-well plate, followed by MRI scanning.

2.4. Experiment 2: Gd compartmentalization

To assess the effects of Gd compartmentalization on T_1 and T_2 relaxation time, five Gd compartmentalization states were compared: viable Gd-liposome-labeled MSCs, non-viable Gd-liposome-labeled MSCs (liposomal as well as cellular membrane lysed), intact Gd liposomes, lysed Gd liposomes and free Gd-DO3A-butrol.

Both lysed cells and lysed liposomes were obtained by repeated freeze–thawing in liquid nitrogen. Cell death was assessed by trypan blue assay, whereas liposomal breakdown was assessed by DLS.

In all *in vitro* experiments stock batches were prepared in Ficoll, preventing cell sedimentation during imaging (12), and a serial dilution was then used to fill a 384-well plate. T_1 and T_2 relaxation times of the top as well as the bottom slice were measured, to make sure sedimentation did not occur. Surrounding wells were filled with water to prevent susceptibility artifacts from air and very concentrated samples.

2.5. MRI data acquisition and analysis

MRI data were acquired at room temperature (20 °C) on a 7 T dedicated animal scanner (Discovery MR901; GE Medical Systems, Milwaukee, IL, USA, and Agilent Technologies, Santa Clara, CA, USA) with unmodified gradients and custom-made surface coils (inner diameter of 5 cm). Spin echo (SE) sequences with multiple *TR* (100–2800 ms; *TE* 10 ms) and multiple *TE* (10–100 ms; *TR* 600 ms) were used to obtain T_1 longitudinal relaxation times and T_2 transverse relaxation times, respectively. Sequences were acquired with field of view (FOV) = 5.0 × 5.0 cm^2, matrix = 160 × 160, slice thickness = 1.4 mm and number of excitations (NEX) = 2. Using MATLAB (version R2007b), T_1 and T_2 times were calculated. Relaxation times were calculated as follows:

$$\Delta R1_{\text{sample}} = \frac{1}{T1_{\text{sample}}} - \frac{1}{T1_{\text{ref}}} \quad (1)$$

in which $T_{1\text{sample}}$ and $T_{1\text{ref}}$ represent the T_1 of the Gd-containing sample of interest and the surrounding wells containing the suspension solution (HEPES or Ficoll), respectively. The same formula was applied to derive ΔR_2 using T_2. $T_{1\text{ref}}$ and $T_{2\text{ref}}$ *in vitro* were assessed to be 3100 ± 120 ms and 167 ± 18 ms, respectively. A voxel-by-voxel linear least-squares fit of the natural logarithm of the signal amplitude versus at least six echo times (*TE*) was performed to construct R_2 maps. For R_1 maps at least six repetition times (*TR*) were used.

2.6. Gd content measurement

The Gd concentration in either liposomes or cells was measured by inductively coupled plasma–optical emission spectroscopy (ICP-OES; Optima 4300DV, Perkin Elmer, Norwalk, CT, USA) operating at a wavelength of 342 nm. Aliquots containing either liposomes or cells were suspended in 4 mL 2% Triton X-100 (St Louis, MO, USA), heated up to 55 °C and mixed for 30 min at 6 *g* to induce cellular and liposomal lysis. For internal validation, stock Gd-DO3A-butrol was included in the measurements as well. This allowed an intergroup comparison of T_1 and T_2 relaxation times, as a function of Gd concentration.

2.7. Statistical analysis

All values are presented as mean ± SD from triplicates and expressed in relation to unlabeled cells.

3. RESULTS AND DISCUSSION

3.1. Experiment 1: the effect of liposomal size and Gd load on signal quenching

T_1 and T_2 relaxation times of a dilution range of the Gd-liposome suspensions (1.0 M_L Gd, 1.0 M_S Gd, 0.6 M_L Gd, 0.6 M_S Gd, 0.3 M_L Gd, 0.3 M_S Gd) were acquired. Assessment of the actual Gd concentration by ICP-OES (Table 1) allowed an intergroup comparison of ΔR_1 and ΔR_2, as a function of Gd concentration. For some of the most concentrated samples the T_1 longitudinal relaxation could not be measured, because it was impossible to fit a curve through these data points; these data points were therefore omitted.

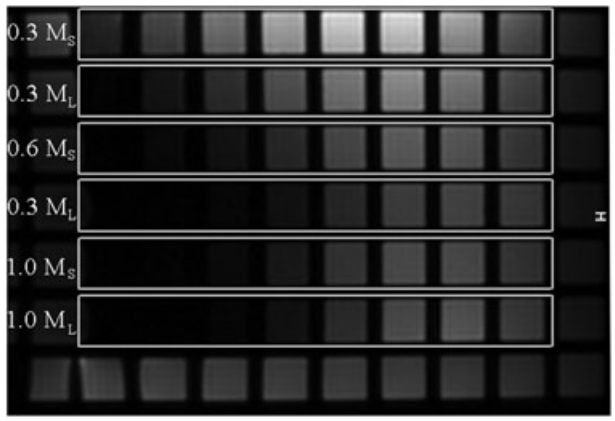

Figure 1. Size- and concentration-dependent contrast effects of Gd liposomes. Experiment 1. T_1-weighted image (*TE* 10 ms, *TR* 400 ms) of a 384-well plate containing a 1:1 serial dilution of various Gd-liposome preparations. Gd liposomes with different intraliposomal [Gd] decreasing in concentration from left to right were scanned. From top to bottom: 0.3 M_S Gd, 0.3 M_L Gd, 0.6 M_S Gd, 0.6 M_L Gd, 1.0 M_S Gd and 1.0 M_L Gd liposomes. The subscripts S and L refer to small and large Gd liposomes, respectively. Note the severe SI loss from highly concentrated samples.

Our data showed that all undiluted samples caused prominent signal hypointensities, except for 0.3 M_S Gd liposomes (Fig. 1). 0.3 M_S liposomes have the highest r_1 relaxivity (i.e. the slope of a linear curve fit through the ΔR_1 data points). Furthermore, the R_1 effects are more pronounced for liposomes with a lower intraliposomal Gd concentration or of a smaller size and for more concentrated liposome suspensions (containing a larger

Table 1. Characteristics of the Gd liposomes and extraliposomal solution

		Liposome type					
		1.0 M_L Gd	1.0 M_S Gd	0.6 M_L Gd	0.6 M_S Gd	0.3 M_L Gd	0.3 M_S Gd
Intraliposomal Gd concentration (M)	$[Gd_l]$	1.0	1.0	0.6	0.6	0.3	0.3
Intraliposomal Gd concentration ($\mu g\,\mu L^{-1}$)	$[Gd_l]$	157	157	94	94	47	47
Liposomal diameter (nm)	$2r_l$	127	83	119	93	124	91
Suspension volume (μL)	V_{tot}	500	470	450	300	300	300
Suspension total Gd mass (μg)[a]	$M_{Gd\ tot}$	14 517	9988	9848	5926	3396	1481
Suspension Gd concentration (mM)	$[Gd_s]$	185	135	139	126	72	31
Volume of single liposome (μL)[b]	V_l	8.39×10^{-13}	2.04×10^{-13}	6.78×10^{-13}	2.99×10^{-13}	7.76×10^{-13}	2.78×10^{-13}
Liposomal Gd mass Gd (μg)	$M_{Gd\ l}$	1.3×10^{-10}	3.2×10^{-11}	6.4×10^{-11}	2.8×10^{-11}	3.7×10^{-11}	1.3×10^{-11}
No of liposomes	N_l	1.1×10^{13}	3.1×10^{13}	1.5×10^{13}	2.1×10^{13}	9.3×10^{12}	1.1×10^{13}
Liposome concentration (μL^{-1})	[L]	2.2×10^{11}	6.6×10^{11}	3.4×10^{11}	7.0×10^{11}	2.5×10^{11}	3.8×10^{11}
Total volume of liposomes (μL)	$V_{l\ tot}$	92	64	105	63	72	31
Total liposomal water volume (μL)[c]	$V_{l\ H2O\ tot}$	64	44	85	51	65	29
Extraliposomal water volume fraction	v_e	0.87	0.91	0.81	0.83	0.78	0.90
Intraliposomal water volume fraction	v_l	0.13	0.09	0.19	0.17	0.22	0.10
Water volume fraction ratio	v_l/v_e	0.15	0.10	0.23	0.21	0.28	0.11
Efflux exchange rate (s^{-1})	κ_{le}	513	822	550	723	526	741
Influx exchange rate (s^{-1})	κ_{el}	88	95	168	188	204	87
Sum of exchange rates (s^{-1})	$\kappa_{le}+\kappa_{el}$	601	917	719	911	730	828
Relaxographic shutter speed (s^{-1})	$\lvert R_{1l}-R_{1e}\rvert$	4200	4200	2520	2520	1260	1260

[a]As measured by ICP-OES.
[b]5 nm membrane thickness subtracted.
[c]Gd-DO3A-butrol (Gadovist) contains 69.33% H_2O

liposome number). Next, the r_1 relaxivity of all Gd-liposome suspensions is lower as compared with uncompartmentalized Gd-DO3A-butrol.

To understand these data we need to take a look at the factors that control r_1 relaxivity, at both the molecular (Gd-chelate) and liposomal levels. As known, interaction of Gd-bound chelates with water protons decreases the water T_1 and T_2 relaxation times. The interactions occurring between Gd and H_2O protons at the molecular level are twofold (13). Inner-sphere relaxation results from the time modulation of the interaction between the magnetic moment of the protons of the water molecules directly coordinated to the metal ion (in the inner coordination sphere) and the magnetic moment of the Gd(III) cations, which results from its unpaired electrons. This interaction of the protons occurs mainly through a dipole–dipole mechanism, and the modulation results from the water exchange rate, the rate of rotational diffusion of the complex and the electron spin relaxation of the Gd(III) ion.

'Outer sphere relaxation' is a more complex concept. It results from the modulation of these dipole–dipole interactions with the protons of the water molecules which diffuse freely near the Gd(III) complex. It is a result of the relative rotational and translational diffusion of water molecules and the paramagnetic ion. Basically stated, the relaxivity influence of the paramagnetic ion enhances when an increased number of water molecules can approach the paramagnetic ion and/or the closer the water protons can approach the paramagnetic ion. The liposomal suspension represents a two-compartment system, where the intraliposomal and the extraliposomal compartments are separated by the liposomal membrane. Gd is contained in the intraliposomal compartment. Diffusion of water across the liposomal membrane thus extends the influence of Gd into the non-contrast-containing compartment. The apparent (measured) voxel SI is *inter alia* dependent on the relaxation rate and the cross-compartmental water exchange rates. As long as the H_2O exchange rate is fast enough on the time scale of T_1, protons excited in one compartment can relax in another compartment (14). The longitudinal relaxation is then in fast exchange. The exchange rates can be derived mathematically. For a single liposome with radius r, with a volume expressed as $V = 4/3\pi r^3$ and surface area as $A = 4\pi r^2$, the unidirectional water efflux rate constant (the reciprocal average liposomal water lifetime) across its membrane can be expressed as (15)

$$\kappa_{le} = \frac{1}{\tau_l} = P_{dl}\frac{A_l}{V_l} = \frac{3P_d}{r_l} \quad (2)$$

P_{dl} (10^{-3}cm^{-1}), representing the diffusional permeability of the liposomal membrane, was derived by interpolation from the nuclear magnetic relaxation dispersion profiles of comparable POPC-liposomes (1-Palmitoyl-2-oleoyl-sn-glycero-3-Phosphocholine), containing 30% cholesterol (16).

The occurring exchange is dependent on both the influx (κ_{el}) and efflux water exchange rates (κ_{le}) and the water volume fraction of the liposomal (v_l) and extraliposomal (v_e) compartments.

The unidirectional water influx rate across the liposomal membrane can thus be expressed as

$$\kappa_{el} = \kappa_{le}\frac{v_l}{v_e} \quad (3)$$

In fast exchange, the apparent voxel relaxation rate will be a weighted average of the relaxation rates of each compartment – independent of the exchange rate, assuming a monoexponential signal recovery (17). This occurs as long as the sum of the exchange rates ($\kappa_{el}+\kappa_{le}$) is much higher than the difference between the compartmental relaxation rates (the relaxographic 'shutter speed') (17,18):

$$\kappa_{el} + \kappa_{le} >> |R_{1l} - R_{1e}| \quad (4)$$

However, if the exchange rate takes on a much smaller value than the difference between the compartmental relaxation rates,

$$\kappa_{el} + \kappa_{le} << |R_{1l} - R_{1e}| \quad (5)$$

the system turns from a fast-exchange to a slow-exchange state (17). In the case of slow exchange, distinct compartmental relaxation times exist, which are dependent on exchange. Liposome-encapsulated Gd represents such a slow-exchange state because of the barrier the liposomal membrane imposes on diffusion, causing the exchange rate of H_2O to be slower than the T_1 proton relaxation time. This hinders an even distribution of the T_1 relaxation time across the entire voxel.

3.1.1. R_1 effects

A dilution range of the Gd liposomes was imaged (Fig. 1). Higher Gd concentrations did not automatically produce higher signal intensities. Instead, all undiluted samples caused prominent signal hypointensities, even on T_1W images, except for 0.3 M_S Gd liposomes. With increasing dilution the SI rises steeply to a certain maximum, followed by a slow decrease in SI. Visually, SI is highest for a fivefold-diluted 0.3 M_S liposome solution (3.9 mM Gd in suspension), as confirmed by the calculated SI (see Fig. 6 later).

The ΔR_1 relaxation rate was plotted against the voxel Gd concentration ([Gd_v]) for each of the six formulations (Fig. 2). The R_1 effects of the intraliposomal Gd concentration, the liposomal size and the liposomal number will be discussed in detail next.

3.1.2. R_1 effects: intraliposomal Gd concentration

At comparable liposomal sizes, 0.3 M Gd liposomes possess a higher r_1 relaxivity than 0.6 M Gd formulations, whereas the latter possess higher r_1 than 1.0 M Gd formulations. This inverted relation might seem paradoxical at first glance. However, it can be clarified by the H_2O availability in proximity to Gd. As previously mentioned, liposome-encapsulated Gd represents a slow-exchange state. Figure 2 indeed confirms that the r_1 relaxivity of all Gd-liposome suspensions is lower than that of uncompartmentalized Gd-DO3A-butrol. In a slow-exchange state the volume distribution of H_2O over the two compartments matters: more specifically, the ratio of the liposomal (v_l) and extraliposomal (v_e) volume water fractions, v_l/v_e (Eq. [3]). The higher r_1 relaxivity of 0.3 M Gd liposomes is attributable to a larger liposomal water volume fraction (v_l), for which, in turn, two reasons may be mentioned. First, compared with suspensions with higher intraliposomal [Gd] ([Gd_l]), a suspension of Gd liposomes with a lower [Gd_l] contains fewer Gd molecules per single liposome and thus more liposomes at equal [Gd_v]. More liposomes means an increase in v_l and a decrease in v_e, increasing v_l/v_e. For example, there are theoretically 3.33 times more liposomes in a suspension of 0.3 M than in a suspension of 1.0 M Gd liposomes. Second, 0.3 M Gd liposomes are created from 1.0 M Gd-DO3A-butrol (containing 69 vol.% H_2O, information acquired through personal communication with Bayer Schering) diluted with HEPES

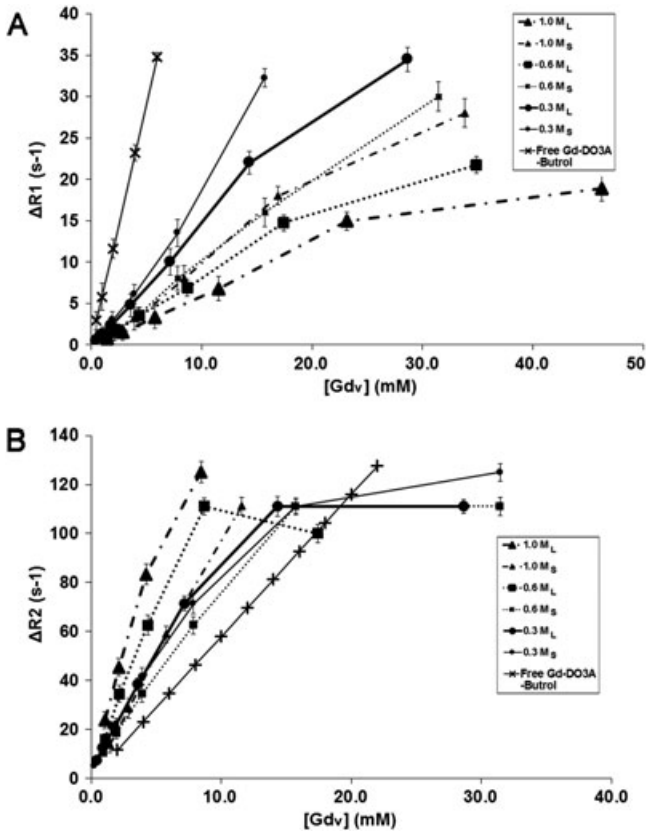

Figure 2. Experiment 1. Line-chart depicting ΔR_1 (A) and ΔR_2 (B) relaxation rates as a function of voxel Gd concentration ($[Gd_v]$) for a range of Gd liposomes with three different intraliposomal [Gd] ($[Gd_l]$), 1.0 M, 0.6 M and 0.3 M Gd. Data are presented as mean ± SD ($n = 3$ different samples; SD refers to intersample SD).

buffer, which contains a higher volume percentage of H_2O (82 vol.% H_2O), additionally increasing v_l by a factor of 1.13 (69% × 0.3 + 82% × 0.7). This totals a net v_l increase by a factor of 3.77 (=3.33 × 1.31). Thus 0.3 M Gd liposomes clearly profit from an increased number of intraliposomal water molecules in the vicinity of Gd-molecules, contributing to the outer sphere effects. The v_l/v_e ratio was calculated by measuring [Gd] in suspension by ICP (from which we derived $[Gd_v]$), using the following equations. Liposomal Gd mass ($M_{Gd\ l}$) can be derived by the product of $[Gd_l]$ (in g L^{-1}) and the single liposomal volume (V_l):

$$M_{Gdl} = [Gd_l]V_l \tag{6}$$

For 1.0 M Gd-DO3A-butrol [Gd] is 157.25 g L^{-1} (as Gd has a molar mass of 157.25 g mol^{-1}). The number of liposomes (N_l) in suspension follows by dividing the total Gd mass in the suspension (after liposomal lysis) ($M_{Gd\ tot}$) by the single liposomal Gd mass ($M_{Gd\ l}$):

$$N_l = \frac{M_{Gdtot}}{M_{Gdl}} \tag{7}$$

Given that the volume percentage of H_2O in undiluted Gd-DO3A-butrol is equal to 69% and the volume percentage of H_2O in HEPES buffer is equal to 82%, the sum of the intraliposomal H_2O volumes of all the liposomes together (V_{ltot}^{H2O}) can be calculated:

$$V_{ltot}^{H2O} = N_l V_l \{0.69 v_{Gd} + 0.82(1 - v_{Gd})\} \tag{8}$$

in which v_{Gd} represents the intraliposomal Gd-DO3A-butrol volume fraction (e.g. 0.6 for 0.6 M Gd liposomes). The liposomal H_2O volume fraction (v_l) can then be derived as follows:

$$v_l = \frac{V_{ltot}^{H2O}}{V_{ltot}^{H2O} + V_{bulk}^{H2O}} = \frac{V_{ltot}^{H2O}}{V_{ltot}^{H2O} + (V_s - V_{ltot})} \tag{9}$$

where V_{bulk}^{H2O} is the total extraliposomal (bulk) volume, V_s is the liposome suspension volume and V_{ltot} the total liposomal volume ($=N_l V_l$). This being an equation of which all parameters are known, v_l was derived. As the total water volume fraction ($v_e + v_l$) is equal to unity, v_l was inputted in the following equation to calculate the water volume fraction ratio of the two compartments:

$$\frac{v_l}{v_e} = \frac{v_l}{1 - v_l} \tag{10}$$

Plotting the water volume fraction ratio v_l/v_e as a function of $[Gd_v]$ shows v_l/v_e indeed to be largest for the 0.3 M Gd liposomes, followed by 0.6 M and 1.0 M Gd liposomes, consecutively (Fig. 3). The increased v_l/v_e ratio increases the water influx exchange rate (κ_{el}). With an unchanged efflux rate (κ_{le}), the sum of exchange rates thus increases, resulting in enhanced T_1 relaxation effects (Eq. (3)).

In addition, 0.3 M Gd liposomes exhibit a relaxographic 'shutter speed' $|R_{1l} - R_{1e}|$ of 1260 s^{-1}, which is 3.33 times lower for than 1.0 M Gd liposomes. Thus the combined effect of the decreased relaxographic 'shutter speed' $|R_{1l} - R_{1e}|$ and increased v_l/v_e ratio drive the 0.3 M Gd liposomes towards a fast-exchange state. The approximation of the rate constants is visible from Fig. 4, where the rate constants are plotted as a function of $[Gd_v]$. The overall effect is an increased higher 'net' voxel r_1 relaxivity for 0.3 M than either 0.6 M or 1.0 M Gd liposomes.

3.1.3. R_1 effects: voxel Gd concentration $[Gd_v]$ or liposome number

The T_1 mapping data (Fig. 2) show the ΔR_1 relaxation rates for all $[Gd_l]$ to increase with an increasing liposome number (i.e. a

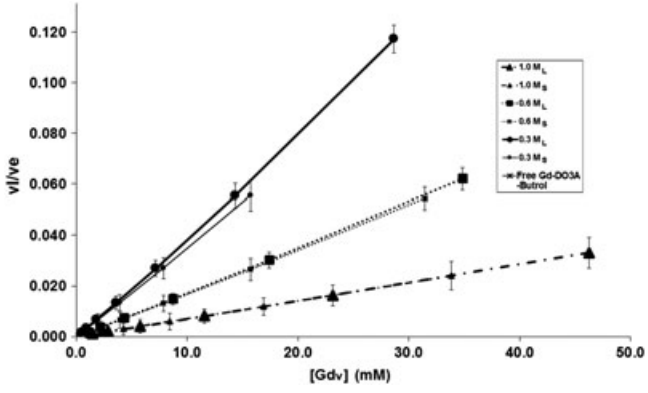

Figure 3. Experiment 1. The ratio of the intraliposomal water volume fraction (v_l) and the extraliposomal bulk water fraction (v_e) was plotted against voxel Gd concentration ($[Gd_v]$). The v_l/v_e ratio is largest for the 0.3 M Gd liposomes, followed by 0.6 M and 1.0 M Gd liposomes, consecutively.

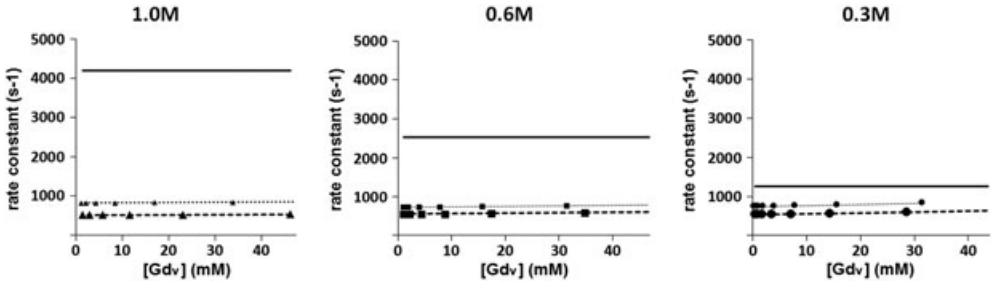

Figure 4. Experiment 1. Rate constants (s^{-1}) of Gd liposomes with an intraliposomal [Gd_l] of 1.0 M, 0.6 M and 0.3 M as a function of the voxel [Gd], [Gd_v]. Undashed lines (– –) represent the relaxographic 'shutter speed' $|R_{1l} - R_{1e}|$, which is the same for small and large liposomes with the same [Gd_l]. The sum of exchange rates ($\kappa_{le} + \kappa_{el}$) of small liposomes is drawn with dotted lines (···), whereas $\kappa_{le} + \kappa_{el}$ for large liposomes is drawn with dashed lines (----). Note the approximation of the rate constants with decreasing intraliposomal [Gd_l]. The approximation of the rate constant $|R_{1l} - R_{1e}|$ and the sum of exchange rates ($\kappa_{le} + \kappa_{el}$) is maximal for 0.3 M Gd liposomes.

higher voxel Gd concentration, [Gd_v]), irrespective of the tested range of [Gd_l]). Again, as mentioned above, an increasing number of liposomes increases the ratio v_l/v_e, thereby increasing the influx rate (κ_{el}) (Eq. [3]). As the liposomal Gd load [Gd_l] remains constant in a serial dilution, $|R_{1l} - R_{1e}|$ remains constant too; this propagates the system towards fast exchange, in agreement with findings by other authors (18). Furthermore, the R_1 curves bend off with increasing voxel [Gd] (Fig. 2), indicating some kind of saturation. The cause for this could lie in the molar ratio H_2O/Gd, which dramatically decreases with increasing liposome number (Fig. 5). In the voxel [Gd] range 0–46 mM a 32-fold decrease in the molar ratio H_2O/Gd occurs, severely lowering the chance of interaction. The maximal intraliposomal H_2O water volume fraction for all undiluted Gd-liposome formulations (0.3–1.0 M) is in the range of 0.1–0.25, so the majority of H_2O molecules are in the extraliposomal free space. This r_1 relaxivity saturation effect should therefore be dominant, especially for the Gd liposomes that are nearest to the fast-exchange regime (0.3 M), as the extraliposomal bulk H_2O really matters in that case because of faster exchange rates.

3.1.4. R_1 effects: liposomal size

Smaller liposomes consistently exhibited a higher r_1 relaxivity than their larger counterparts (Fig. 2). The explanation for this is straightforward. As a result of the larger surface to volume ratio, smaller liposomes have a higher efflux rate (κ_{le}) (Eq. [2]). This augments the sums of exchange rates, contributing to faster exchange.

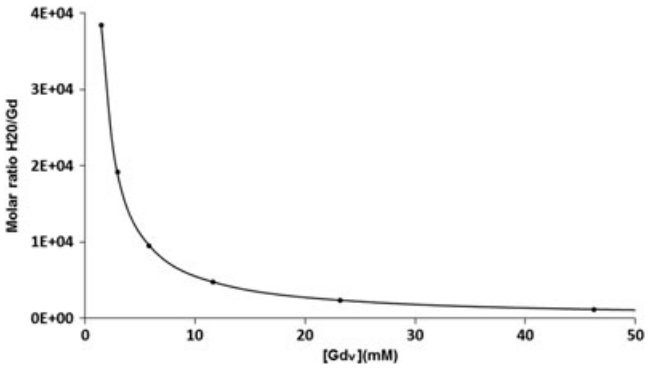

Figure 5. Experiment 1. The molar ratio H_2O/Gd of an arbitrary Gd-liposome suspension is calculated and plotted as a function of the voxel Gd concentration ([Gd_v]). The molar ratio H_2O/Gd decreases exponentially with an increasing [Gd_v], which may account for the lower interaction chance of H_2O with Gd atoms, and contribute to the 'R_1 saturation' occurring with increasing [Gd_v] (see Fig. 2).

3.1.5. R_2 effects

In many studies on compartmentalized Gd contrast agents to date, the effect on R_2 relaxation rate was not considered. However, Gd-based contrast agents have a biphasic effect on SI dependent on the concentration and can introduce a T_2 effect (severe signal loss) at high concentrations, even on T_1-weighted pulse sequences.

In our study for all Gd liposomes, r_2 relaxivity was higher than for free Gd. This is explained by the more heterogeneous distribution of liposomal encapsulated Gd atoms across the voxel, increasing the local magnetic susceptibility differences, which in turn lead to intravoxel dephasing. Furthermore, R_2 relaxation rates increased according to the liposomal Gd load [Gd_l]; i.e., the higher the intraliposomal Gd load the higher the r_2 relaxivity (i.e. the slope of a linear curve fit through the ΔR_2 data points) (Fig. 2). This can be explained by the lower number of liposomes in suspensions with high [Gd_l], causing more heterogeneity (see Table 1, 1.0 M_L have the lowest [liposomes], 2.21×10^{10}). For similar [Gd_l], the r_2 relaxivity was higher for larger liposomes, presumably owing to the lower number of larger liposomes per voxel at similar [Gd_v], resulting in a more heterogeneous distribution of spin moments across the voxel. These findings are important, as the SI or perceived final contrast is dictated by both R_1 and R_2 effects. In addition, being aware of the intravoxel dephasing effect allows us to choose the optimal MRI sequence, according to the desired outcome. SE sequences can reverse this effect by a 180 degree inversion pulse; a gradient-echo sequence cannot.

3.1.6. Combined R_1 and R_2 effects: SI

Differences in concentration of compartmentalized Gd can generate contrast effects across the entire range from hypo- to hyperintensity (Fig. 1). Considering this versatility of Gd liposomes, it is essential to be informed about the dose response of the SI. Having shown that compartmentalization affects T_1 as well as T_2 relaxation times, both parameters need to be taken into account. SI for an SE sequence is described by (19)

$$SI = M_z\left(1 - e^{-TR/T1}\right)e^{-TE/T2} \quad (11)$$

A simulated dose response curve of the tested Gd liposomes in a typical SE sequence (*TR* 500, *TE* 10 ms) was generated for

all Gd liposomes (Fig. 6). Initially T_1 relaxation dominates, but as the CA concentration becomes sufficiently high T_1 saturation as well as counter-acting T_2 relaxation becomes dominant, resulting in signal loss at higher concentrations. There is significant SI quenching for all Gd liposomes, compared with free Gd-DO3A-butrol. Compared with free Gd-DO3A-butrol the curves for Gd liposomes are shifted to the right, attaining their maximal SI at higher voxel [Gd]. Of all liposomes, 0.3 M small Gd liposomes (91 nm) achieve the highest SI, closely followed by larger liposomes (124 nm) with the same [Gd_l]. As previously explained, the R_1 effects underlying this are a result of the combination of the decreased relaxographic 'shutter speed' $|R_{1l} - R_{1e}|$, the increased sum of exchange rates ($\kappa_{le} + \kappa_{el}$) (due to the increased ratio v_l/v_e resulting from an increased liposome number) and lower R_2 effects because of lower field inhomogeneities.

Understanding these effects allows one to titrate the optimal intraliposomal ([Gd_l]) and voxel Gd concentration ([Gd_v]) according to the needs and desired application for a specific MRI sequence.

3.2. Experiment 2: the effect of compartmentalization state on signal quenching

To assess the effect of the extent of compartmentalization, five different compartmentalization states of Gd were compared *in vitro*: viable Gd-liposome-labeled MSCs, lysed (non-viable) Gd-liposome-labeled MSCs, intact Gd liposomes, lysed Gd liposomes and free Gd-DO3A-butrol. Taking into consideration the high voxel [Gd] ([Gd_v]) for stock liposomes, a large number of cells was required ($>10 \times 10^7$) to allow for intergroup comparisons to be made. The range of [Gd_v] is therefore smaller than for Experiment 1 (Fig. 7).

3.2.1. R_1 effects

Gd compartmentalization in either a liposomal or a cellular–liposomal form reduces r_1 longitudinal relaxivity as compared with free Gd-DO3A-butrol (Fig. 7). In parallel, the r_1 relaxivity in the lysed groups (lysed cells or lysed liposomes) was larger than the r_1 of the intact groups (intact cells or intact liposomes). The main reason for this lies in the fact that after lysis of the cell and/or liposome membrane an important barrier between bulk H_2O molecules and Gd is abrogated. The r_1 relaxivity for the lysed groups though still remains slightly lower than for free Gd-DO3A-butrol. A presumable cause could be found in the fact that the solution contains an additional amount of liposomal and cellular debris, posing a remaining barrier for H_2O molecules in their diffusional pathways.

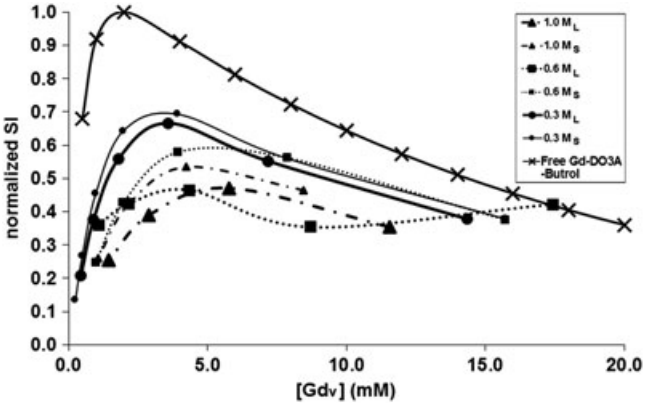

Figure 6. Experiment 1. Simulated dose response of Gd liposomes with varying intraliposomal Gd concentration. Typical SE sequence (*TR* 500, *TE* 10 ms) as a function of the voxel Gd concentration, [Gd_v]. Initially T_1 relaxation dominates, but as the CA concentration becomes sufficiently high T_1 saturation as well as counter-acting T_2 relaxation becomes dominant, resulting in signal loss at higher concentrations. There is significant SI quenching for all Gd liposomes throughout the entire concentration range tested, compared with free Gd-DO3A-butrol. The highest SI of all liposomes is achieved by 0.3 M small Gd liposomes (91 nm), closely followed by larger liposomes (124 nm) with the same [Gd_l].

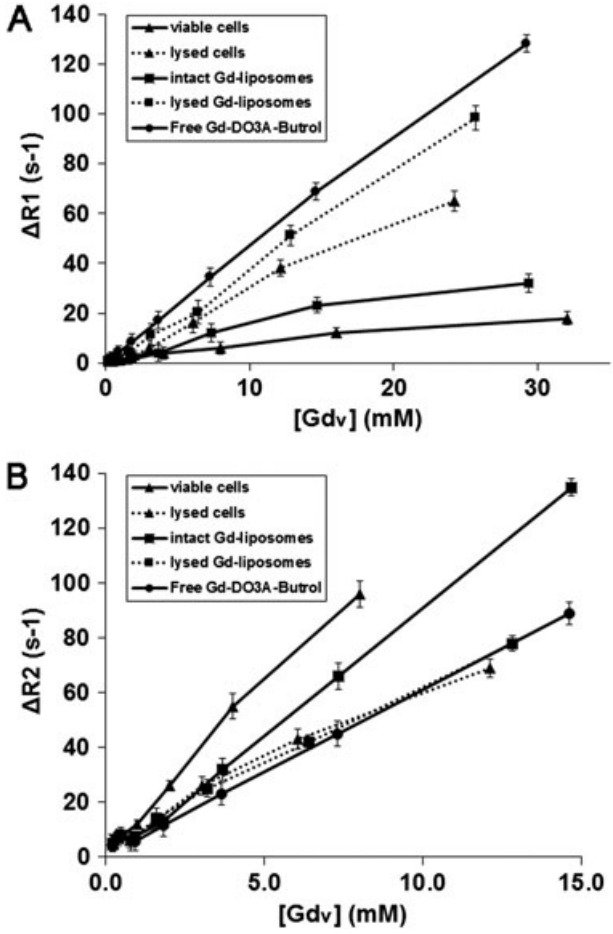

Figure 7. Experiment 2. Line-chart depicting the effect of compartmentalization on ΔR1 (A) and ΔR2 (B) relaxation rate as a function of voxel Gd concentration ([Gd < sub > v</sub>]) of several different Gd-suspensions (1.0 M): viable Gd-liposome-labeled MSCs, non-viable Gd-liposome-labeled MSCs, intact Gd liposomes, ruptured Gd liposomes and free Gd-DO3A-butrol. Data are presented as mean ± SD (n = 3 different samples, SD refers to intersample SD).

3.2.2. R_2 effects

Compartmentalization of Gd, in both liposomes and cells, increases the r_2 relaxivity (Fig. 7), compared with free Gd-DO3A-butrol. This is in accordance with the findings in Experiment 1. Again, this can be explained by the heterogeneous distribution of Gd across the voxel in compartmentalized form, increasing the local magnetic susceptibility differences leading to intravoxel dephasing. The r_2 relaxivity for Gd liposomes in viable (intact)

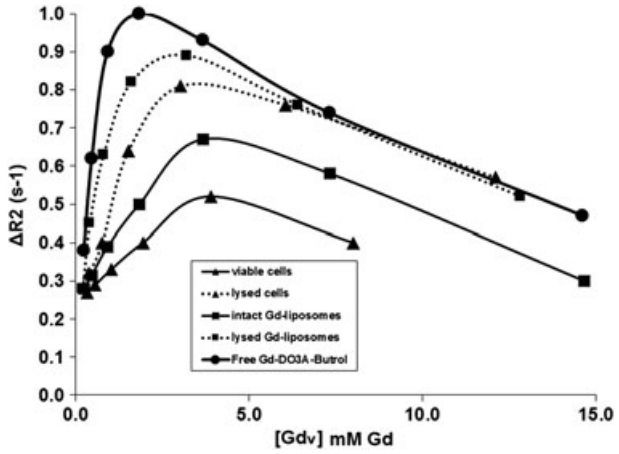

Figure 8. Experiment 2. Simulated dose response of Gd liposomes in various compartmentalization states. Typical SE sequence (TR 500, TE 10 ms) as a function of the voxel Gd concentration, [Gd < sub > v</sub>]. Similar to Fig. 2, T2 relaxation results in signal loss at higher concentrations. There is significant SI quenching for all compartmentalization states, compared with free Gd-DO3A-butrol.

cells was larger than for intact liposomes. Presumably, the clustering of Gd liposomes inside cells leads to a more heterogeneous suspension than a suspension containing mere Gd liposomes, in which the liposomes can diffuse.

3.2.3. *Combined R_1 and R_2 effects: SI*

Similar to Experiment 1, a simulated dose-dependent SI curve of the five compartmentalization groups of Gd liposomes was generated for a typical SE sequence (*TR* 500, *TE* 10 ms) (Fig. 8). Naturally, free Gd-DO3A-butrol performs best with regard to the maximum SI, closely followed by lysed Gd liposomes. Lysed Gd liposomes outperform lysed Gd-liposome-labeled cells in SI, obviously because of a slightly larger R_1 effect. A lysed state performs better in reaching a high SI (for both liposomes and cells) than an intact state, because of the combination of an increased R_1 and a decreased R_2 effect.

A limitation to take into account in this study is the fact that the intraliposomally present Gd-DO3A-butrol causes hypertonicity. This might have led to a [Gd_i] that is smaller than the assumed one, with consequent effects on the r_1 relaxivity. Although we were aware of this, liposomes were still suspended in an isotonic suspension, to simulate the cell-labeling environment as best as possible. A hypertonic liposomal suspension has no place in cell labeling for two reasons: first because the hypertonicity would quickly progress to near-isotonicity, as a small liposomal suspension volume would distribute over a much larger cell culture volume; trying to overcome this by rendering the cell culture volume hypertonic would be useless, as it would induce cell shrinkage and cell death.

Furthermore, with regard to the P_{dl} value in Eq. [2], we used liposomes with 33% cholesterol in a mixture of DPPC:cholesterol: DOTAP in the molar ratio 47:33:20, whereas the P_{dl} value taken from the referred article was derived from POPC liposomes with 30% cholesterol. As cholesterol is the most important constituent of all three lipids in defining the liposomal permeability, we think the setup is comparable. However, there is some uncertainty with regard to this.

4. CONCLUSIONS

Internalization of Gd liposomes has proven to be an efficient way to load cells with Gd (1,10,20). However, Gd can exhibit a dynamic contrast behavior, eliciting a contrast effect anywhere in the range from hypo- to hyperintensity. This can be used advantageously as a qualitative measure of cell viability (11). As Gd can induce quenching effects as a result of either compartmentalization, liposome size, intraliposomal Gd concentration or R_2 effects, we studied the relation between these parameters and SI. Since the main effort in MRI-based cell tracking with Gd is to augment the sensitivity (21), e.g. by achieving a high payload of Gd per cell or a high r_1 relaxivity of the Gd contrast agent used, we directed special interest to the high Gd concentration range (0.3–1.0 M Gd). We show here that an increasing intraliposomal Gd concentration (>0.3 M Gd) has a deteriorating effect on SI, due to both a reduced r_1 and increased r_2 relaxivity. Internalization of the Gd chelates into liposomes creates an intraliposomal compartment with large r_1 but small volume fraction and an extraliposomal compartment with large volume fraction but small r_1. The final voxel SI will thus be a combined result of the influx and efflux H_2O rates, the H_2O volume fraction ratio of the compartments and R_2 effects. Compartmentalization of Gd liposomes in cells further compromises the maximum achievable SI.

Four main conclusions can be drawn.

(1) Suspensions of Gd liposomes with a lower intraliposomal [Gd] benefit from a higher v_i/v_e ratio (liposomal /extraliposomal H_2O volume fraction), a lower relaxographic 'shutter speed' $|R_{1i} - R_{1e}|$ and a lower R_2 effect, resulting in less signal quenching. Less is more. However, even for the less concentrated 0.3 M Gd liposomes, the water exchange rate across the liposomal membrane is still not high enough to distribute this high relaxivity over the entire voxel, resulting in signal quenching compared with free Gd.
(2) Smaller liposomes gain higher r_1 relaxivity and higher SI due to the larger surface-to-volume ratio, resulting in a larger efflux H_2O rate (κ_{ie}). Consequently, water exchange across the liposomal membrane is more efficient, leading to a reduced quenching effect.
(3) Concentrated liposome suspensions, i.e. those containing high numbers of liposomes, are characterized by large R_2 effects and reduced R_1 effects, resulting in more signal quenching.
(4) Compared with free Gd, compartmentalized Gd (in liposomes or cells) suffers from a decreased R_1 and increased R_2 effect, inducing signal loss and thus significantly contributing to the quenching effect. Especially in cell labeling studies where efforts are undertaken to augment Gd sensitivity, this effect needs to be taken into account. On the other hand, the versatility of contrast generation by encapsulated Gd can serve as a tool for read-out of functional cell status, since viable and lysed cells generate different contrasts (10).

Understanding the underlying principles that lead to the observed results (i.e. the interplay between intra- and extraliposomal water fractions, the difference between the intra- and extraliposomal relaxation rates and the increased R_2 effect as a result of compartmentalization) allows one to tailor the optimal liposomal Gd concentration according to the desired goal.

REFERENCES

1. Guenoun J, Koning GA, Doeswijk G, Bosman L, Wielopolski PA, Krestin GP, Bernsen MR. Cationic Gd-DTPA liposomes for highly efficient labeling of mesenchymal stem cells and cell tracking with MRI. Cell Transpl 2012; 21(1): 191–205.
2. Biancone L, Crich SG, Cantaluppi V, Romanazzi GM, Russo S, Scalabrino E, Esposito G, Figliolini F, Beltramo S, Perin PC, Segoloni GP, Aime S, Camussi G. Magnetic resonance imaging of gadolinium-labeled pancreatic islets for experimental transplantation. NMR Biomed 2007; 20(1): 40–48.
3. Geninatti Crich S, Cabella C, Barge A, Belfiore S, Ghirelli C, Lattuada L, Lanzardo S, Mortillaro A, Tei L, Visigalli M, Forni G, Aime S. In vitro and in vivo magnetic resonance detection of tumor cells by targeting glutamine transporters with Gd-based probes. J Med Chem 2006; 49(16): 4926–4936.
4. Ghaghada K, Hawley C, Kawaji K, Annapragada A, Mukundan S Jr. T1 relaxivity of core-encapsulated gadolinium liposomal contrast agents – effect of liposome size and internal gadolinium concentration. Acad Radiol 2008; 15(10): 1259–1263.
5. Lewin M, Clement O, Belguise-Valladier P, Tran L, Cuenod CA, Siauve N, Frija G. Hepatocyte targeting with Gd-EOB-DTPA: potential application for gene therapy. Invest Radiol 2001; 36(1): 9–14.
6. Strijkers GJ, Mulder WJ, van Heeswijk RB, Frederik PM, Bomans P, Magusin PC, Nicolay K. Relaxivity of liposomal paramagnetic MRI contrast agents. Magn Reson Mater Phys Biol Med 2005; 18(4): 186–192.
7. Terreno E, Geninatti Crich S, Belfiore S, Biancone L, Cabella C, Esposito G, Manazza AD, Aime S. Effect of the intracellular localization of a Gd-based imaging probe on the relaxation enhancement of water protons. Magn Reson Med 2006; 55(3): 491–497.
8. Billotey C, Wilhelm C, Devaud M, Bacri JC, Bittoun J, Gazeau F. Cell internalization of anionic maghemite nanoparticles: quantitative effect on magnetic resonance imaging. Magn Reson Med 2003; 49(4): 646–654.
9. Brekke C, Morgan SC, Lowe AS, Meade TJ, Price J, Williams SC, Modo M. The *in vitro* effects of a bimodal contrast agent on cellular functions and relaxometry. NMR Biomed 2007; 20(2): 77–89.
10. Guenoun J, Ruggiero A, Doeswijk G, Janssens RC, Koning GA, Kotek G, Krestin GP, Bernsen MR. *In vivo* quantitative assessment of cell viability of gadolinium or iron-labeled cells using MRI and bioluminescence imaging. Contrast Media Mol Imaging 2013; 8(2): 165–174.
11. Rouser G, Fkeischer S, Yamamoto A. Two dimensional then layer chromatographic separation of polar lipids and determination of phospholipids by phosphorus analysis of spots. Lipids 1970; 5(5): 494–496.
12. Sutton EJ, Henning TD, Boddington S, Demos S, Krug C, Meier R, Kornak J, Zhao S, Baehner R, Sharifi S, Daldrup-Link H. In vivo magnetic resonance imaging and optical imaging comparison of viable and nonviable mesenchymal stem cells with a bifunctional label. Mol Imaging 2010; 9(5): 278–290.
13. Sattler KD. Handbook of Nanophysics. Nanomedicine and Nanorobotics. Taylor and Francis: Boca Raton, FL, 2009.
14. Bauer WR, Schulten K. Theory of contrast agents in magnetic resonance imaging: coupling of spin relaxation and transport. Magn Reson Med 1992; 26(1): 16–39.
15. Chen ST, Springer CS Jr. Ionophore-catalyzed cation transport between phospholipid inverted micelles manifest in DNMR. Biophys Chem 1981; 14(4): 375–388.
16. Koenig SH, Ahkong QF, Brown RD III, Lafleur M, Spiller M, Unger E, Tilcock C. Permeability of liposomal membranes to water: results from the magnetic field dependence of T_1 of solvent protons in suspensions of vesicles with entrapped paramagnetic ions. Magn Reson Med 1992; 23(2): 275–286.
17. Donahue KM, Weisskoff RM, Burstein D. Water diffusion and exchange as they influence contrast enhancement. J Magn Reson Imaging 1997; 7(1): 102–110.
18. Strijkers GJ, Hak S, Kok MB, Springer CS Jr, Nicolay K. Three-compartment T_1 relaxation model for intracellular paramagnetic contrast agents. Magn Reson Med 2009; 61(5): 1049–1058.
19. Yamada S, Matsuzawa T, Yamada K, Yoshioka S, Ono S, Hishinuma T. A modified signal intensity equation of Carr–Purcell–Meiboom–Gill pulse sequence for MR imaging. Tohoku J Exp Med 1989; 158(3): 203–209.
20. Kok MB, Hak S, Mulder WJ, van der Schaft DW, Strijkers GJ, Nicolay K. Cellular compartmentalization of internalized paramagnetic liposomes strongly influences both T_1 and T_2 relaxivity. Magn Reson Med 2009; 61(5): 1022–1032.
21. Aime S, Castelli DD, Crich SG, Gianolio E, Terreno E. Pushing the sensitivity envelope of lanthanide-based magnetic resonance imaging (MRI) contrast agents for molecular imaging applications. Acc Chem Res 2009; 42(7): 822–831.